Chromosomal Duplication Involving the Forkhead Transcription Factor Gene *FOXC1* Causes Iris Hypoplasia and Glaucoma

Ordan J. Lehmann,[1] Neil D. Ebenezer,[1] Tim Jordan,[1,5] Margaret Fox,[2] Louise Ocaka,[1] Annette Payne,[1] Bart P. Leroy,[1] Brian J. Clark,[4] Roger A. Hitchings,[3] Sue Povey,[2] Peng T. Khaw,[3] and Shomi S. Bhattacharya[1]

[1]Department of Molecular Genetics, Institute of Ophthalmology, [2]MRC Human Biochemical Genetics Unit, Galton Laboratory, University College, [3]Moorfields Eye Hospital, and [4]Department of Pathology, Institute of Ophthalmology, London; and [5]Eye Unit, Southampton General Hospital, Southampton

The forkhead transcription factor gene *FOXC1* (formerly *FKHL7*) is responsible for a number of glaucoma phenotypes in families in which the disease maps to 6p25, although mutations have not been found in all families in which the disease maps to this region. In a large pedigree with iris hypoplasia and glaucoma mapping to 6p25 (peak LOD score 6.20 [recombination fraction 0] at D6S967), no *FOXC1* mutations were detected by direct sequencing. However, genotyping with microsatellite repeat markers suggested the presence of a chromosomal duplication that segregated with the disease phenotype. The duplication was confirmed in affected individuals by FISH with markers encompassing *FOXC1*. These results provide evidence of gene duplication causing developmental disease in humans, with increased gene dosage of either *FOXC1* or other, as yet unknown genes within the duplicated segment being the probable mechanism responsible for the phenotype.

Introduction

The glaucomas are a heterogeneous group of disorders that are characterized by an optic neuropathy in which retinal ganglion cell death leads to excavation of the optic-nerve head and to visual field loss. They are responsible for >6 million cases of blindness and represent the second most common cause of visual loss worldwide (Quigley 1996). On the basis of population surveys, it is estimated that ⩾20% of glaucoma cases have a genetic basis (Wolfs et al. 1998), although evidence suggests that this is a conservative figure (Alward et al. 2000; Mackey et al. 2000). The genetic heterogeneity of the inherited glaucomas is illustrated by the number of mapped loci and the number of glaucoma-causing genes (*PITX2* [MIM 601542], *MYOC* [MIM 601652], *CYP1B1* [MIM 601771], *LMX1B* [MIM 602575], and *FOXC1* [MIM 601090]) that have been identified so far (Craig et al. 1999).

Mutations in the forkhead transcription factor gene *FOXC1* cause a range of developmental anomalies associated with glaucoma, including Axenfeld anomaly, Rieger anomaly, iris hypoplasia, and Rieger syndrome (Nishimura et al. 1998; Mirzayans et al. 2000). These phenotypes have been reported both in isolated cases and in pedigrees in which an autosomal dominant pattern of inheritance is observed. However, four such pedigrees that map to 6p25 do not contain a mutation in the coding region of the *FOXC1* gene (Jordan et al. 1997; Morissette et al. 1997; Mears et al. 1998). In two of these families, *FOXC1* has been excluded from the disease-causing interval, by mapping data based on recombination events. These findings suggest the existence of a second glaucoma-causing gene on 6p25 (Mears et al. 1998). In this article, we report the mapping of a large, previously unreported pedigree with iris hypoplasia and glaucoma, in which a chromosomal duplication event involving *FOXC1* appears to be responsible for the phenotype.

Subjects and Methods

Family and Clinical Data

The family presented has an autosomal dominantly transmitted form of iris hypoplasia and glaucoma that can be traced back six generations. The family includes 21 living affected individuals, of whom 18 were ascertained, together with 9 unaffected siblings and 9 spouses (fig. 1*a*). The study had the approval of the Moorfields Eye Hospital ethics committee, and informed consent was obtained from all participants.

Clinical examination (performed by O.J.L. and T.J.) included portable slit-lamp biomicroscopy, gonioscopy, disk examination, and anterior-segment photography.
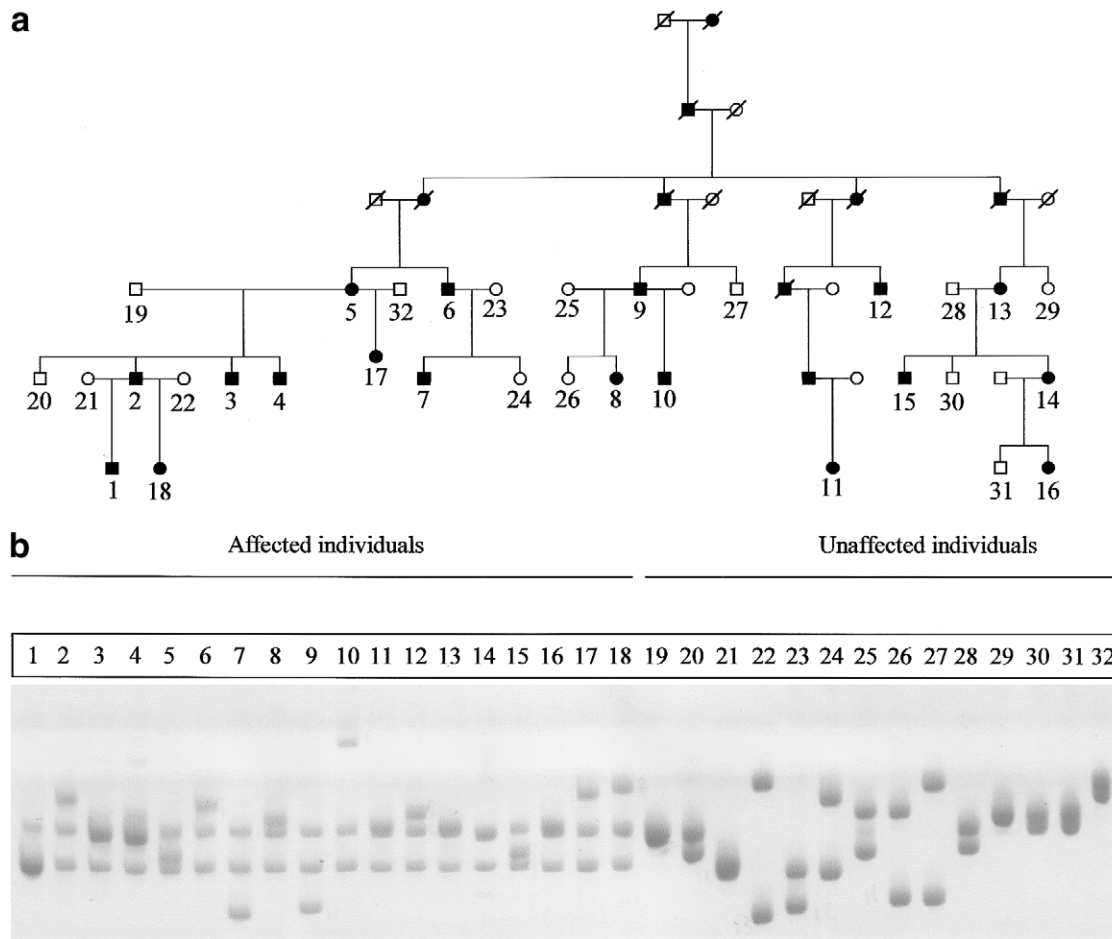
Figure 1   *a,* Abridged pedigree drawing illustrating the affected (1–18) and the unaffected (19–31) individuals analyzed. *b,* Photograph of ethidium-bromide–stained gel, showing D6S967 PCR products. Each lane number corresponds with that of the individual in the pedigree in *a.*

All affected family members had marked hypoplasia of the iris stroma, which had been apparent since birth, and a prominent sphincter pupillae (fig. 2*A* and *C*). An anomalous angle configuration with an anterior iris insertion and/or an increased number of iris strands was present in the majority of individuals, although this could not be accurately assessed in individuals who had undergone goniotomy during infancy. The clinical finding of iris hypoplasia was the criterion used to assign an individual's affected status. Patients' ophthalmic records were obtained and used to confirm the ophthalmic history. Glaucoma (diagnosed by the combination of optic-disk cupping and visual field loss) was present in all 18 affected individuals who could be fully examined, and the age at onset was generally during the 1st decade of life (range 0–18 years). The clinical finding of iris atrophy was confirmed by histological examination of a peripheral iridectomy specimen collected from individual 1 during glaucoma surgery (fig. 2C). No dental

or umbilical abnormalities were present in affected individuals.

Genotyping and Linkage Analysis

Genomic DNA was extracted, from either venous blood or buccal mucosa samples, from 32 individuals, by standard techniques (Qiagen, Nucleon Biosciences). Each DNA sample was subjected to 35 cycles of PCR amplification using microsatellite tri-/tetranucleotide-repeat markers in 20-μl reaction volumes (20 ng genomic DNA, 10 pmol of each primer, 200 mM of each dNTP, 1.5 mM MgCl, and 2 units of *Taq* DNA Polymerase [Promega]). The microsatellite markers (D6S1600, D6S942, D6S967, D6S344, D6S1713, and D6S1574 [all from Research Genetics]) were amplified by 35 cycles of 94°C for 1 min, 55°C for 1 min, and 72°C for 1 min. The amplified PCR products were separated by 6% nondenaturing PAGE (Protogel) and were visualized by staining with ethidium bromide. Subsequent genotyping was done manually.
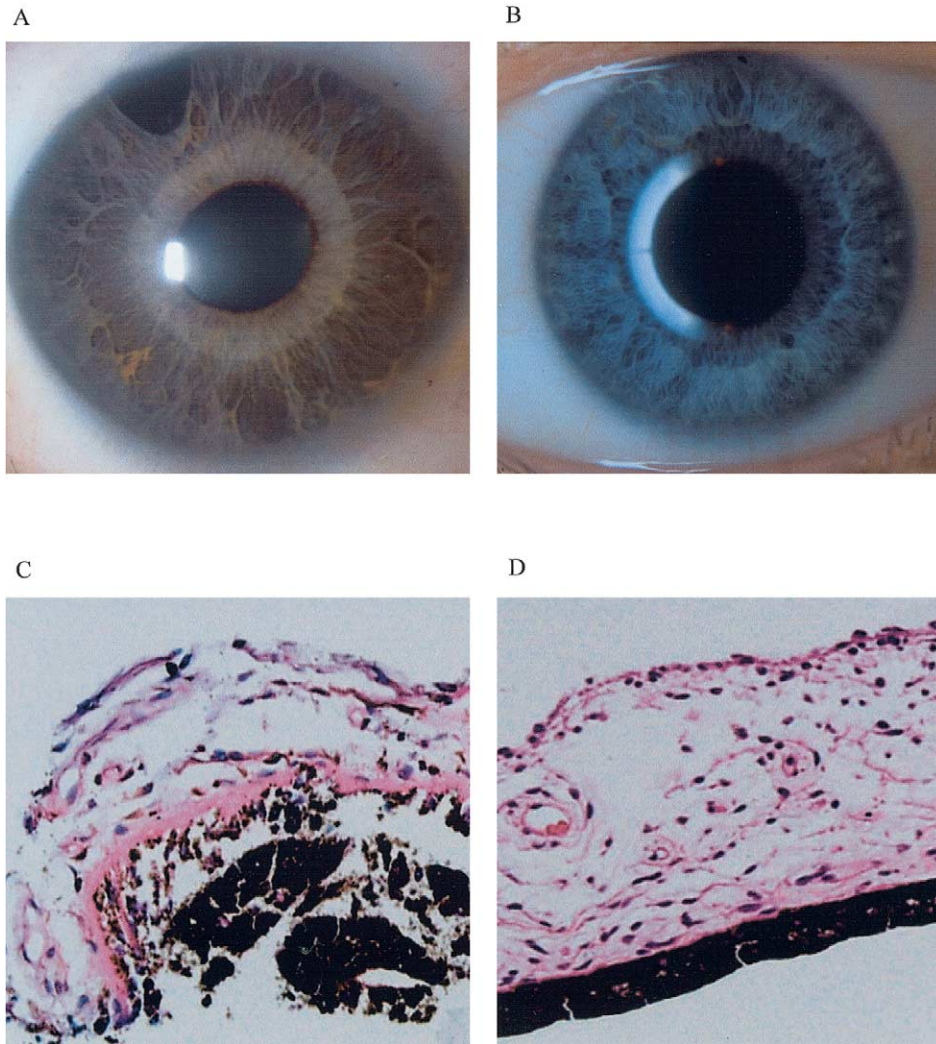
Figure 2   Ocular anterior-segment photographs and iris histology micrographs from members of the pedigree and normal controls. *A,* Left eye of individual 3, displaying the characteristic iris stromal atrophy, with exposure of the underlying iris sphincter visible as a pale ring encircling the pupil. A surgical iridectomy is present. *B,* Left eye of unaffected individual (individual 20); the semicircular light reflex is a corneal reflection from the ring flash. *C,* Micrograph of iris specimen (individual 1), confirming that the reduction in iris thickness to ∼150 μm was due primarily to a reduction in stromal thickness. At its thinnest, the iris consists of little more than the thickness of the dilator muscle alone, and elsewhere the thinned stroma contained normal blood vessels and was of normal cellular density. (Separation of the posterior pigment epithelium from the iris stroma is a surgical artifact). *D,* Micrograph of normal iris, for comparison (thickness ∼350 μm).

Two-point linkage analysis was performed using the MLINK component of the LINKAGE program, version 5.1 (Lathrop and Lalouel 1984), with an autosomal dominant model, 100% penetrance, a gene frequency of .0001 and a mutation rate of .00001 (table 1). Because the phenotype is apparent during infancy, no age correction for penetrance was required.

Mutation Detection

PCR amplification of *FOXC1* and *FOXF2* gene sequences was performed in 20-μl reactions at an annealing temperature of 60°C, by a modification of published methodology (Mears et al. 1998) in which 10% glycerol and 5% formamide were substituted for DMSO, to alleviate the problems associated with amplification of GC-rich sequences. The *FOXC1* and *FOXF2* primer sequences used are shown in table 2 (Mears et al. 1998). After purification with QIAquick columns (Qiagen), under standard conditions, samples were sequenced bidirectionally with fluorescent dideoxynucleotides (PE Biosystems) on an ABI 373 automated sequencer.

FISH

As part of a positional cloning approach, a YAC/PAC contig spanning *FOXC1* was established: YACs 870D6

Table 1

Two-Point LOD Scores between the Iris Hypoplasia Locus and Six Markers on 6p25

	LOD Score at $\theta =$					
Locus	.00	.05	.10	.20	.30	.40
D6S1600	0	.66	.22	.73	.69	.41
D6S942	$-\infty$	3.90	3.68	2.86	1.84	.78
D6S967	6.20	5.65	5.08	3.87	2.56	1.20
D6S344	1.45	1.36	1.23	.87	.50	.20
D6S1713	5.3	4.98	4.50	3.31	2.92	1.44
D6S1574	$-\infty$	2.17	2.19	1.78	1.16	.50

and 905F3 were from the database of the Whitehead Institute for Biomedical Research/MIT Center for Genome Research; PACs dJ118B18, dJ181K4, dJ181D15, dJ183B12, and dJ135A7 were isolated by screening the RPCI1 library with D6S344. To confirm that PACs contained *FOXC1,* STS (sequence-tagged site) content mapping was performed with *FOXC1*-specific primers.

Metaphase-chromosome preparations were obtained from short-term peripheral blood cultures of individuals 13 and 14 and of a normal control, by standard methods. PAC 135A7 (chromosome 6p25) and PAC 124L22 (chromosome 2q21) (also derived from the RPCI1 library), labeled, by nick translation, with biotin and digoxygenin, respectively, were used as probes for FISH. The probes were simultaneously hybridized to metaphase and interphase nuclei from the three individuals. The signals were detected using fluorescein isothiocyanate avidin for biotin and rhodamine antidigoxygenin, as described elsewhere (Fox and Povey 2000). The signals were analyzed using fluorescent microscopy and were imaged by cooled CCD (Photometrics) and Smartcapture software (Vysis).

Results

Positive LOD scores were obtained for markers on chromosome 6p25. The maximum two-point LOD score of 6.20 (recombination fraction 0) was obtained with D6S967; recombination events at D6S942 and D6S1713 define the ~6-cM disease-gene–containing interval. The markers and two-point LOD scores are shown in table 1.

Unusual genotyping results were obtained with marker D6S967, which suggests the presence of a duplication event. All affected individuals shared two D6S967 alleles of consistent size across the pedigree and displayed an extra allele either as a third band (individuals 2, 5–10, 12, 15, 17, and 18) or as an allele band of twice-normal signal intensity (fig. 1*b*). PCR products from representative alleles were extracted from the gel and were sequenced bidirectionally to confirm these findings (data not shown). No other microsatellite markers exhibited this phenomenon. Direct sequencing of *FOXC1* and *FOXF2* demonstrated that no mutations were present in these genes. FISH was performed to confirm the duplication event observed with D6S967.

The majority of metaphase preparations from affected individuals contained a hybridization signal on chromosome 6p25, in which one homologue contained a brighter signal than its partner (individual 13, 6 of 9; individual 14, 9 of 11; control individual, 1 of 6). In contrast, signals of PAC 124L22 (2q21) were mainly of similar intensity, the number of unequal signals being as follows: individual 13, 1 of 9; individual 14, 2 of 11; control individual, 2 of 6. The chromosome morphology of the two homologues at 6p25 appeared indistinguishable. Examination of 239 interphase-nuclei preparations from both affected individuals (119 from

Table 2

Sequences of Primer Pairs Used in PCR Amplification of *FOXC1* and *FOXF2*

| Gene	Forward Primer (5′→3′)	Reverse Primer (5′→3′)
FOXC1	ACCACCCTGCGGCCCACCAAG	CGGAGACCTGGGCCACTTGGC
	CCCGGACTCGGACTCGGC	CCGAGGTAGGGCACCACT
	GTCCAGCCCCAACTCCCT	GCATGGCGGTGTAGCC
	GGCTACACCGCCATGC	ACTGGTAGATGCCGTTCAGG
	GGCGCTTCAAGAAGAAGGAC	CTGAAGCCCTGGCTATGGT
	AAGATCGAGAGCCCCGAC	CAGAAGGCCGGAGCTGAG
	ACCATAGCCAGGGCTTCAG	CAGGTTGCAGTGGTAGGTCC
	CAAGCCATGAGCCTGTACG	GGGTTCGATTTAGTTCGGCT
FOXF2	CTGGGAGGCCGTTGCGCAAGGCAG	CGCTCCAGGCCGCCCTGATGAGC
	CGCTCCAGGCCGCCCTGATGAGC	CTCGGTGCGCCACAATCTCTC
	CTCGCCCAGCAAGCGCCTGACG	GGCTTCGACTTCCAGGCGCCC
	CGGAAGTGCCAGGCGCTCAAG	AGCCCGGTACCCTCGTCCCCG
	CTGCCCGGTGCCCGCGGGACCCG	CTGGCGGCCACTGCCACTCCCAC
	CACCCTGCCATCCACTGGATGAC	GAGGGGGCAGATAGAAAC
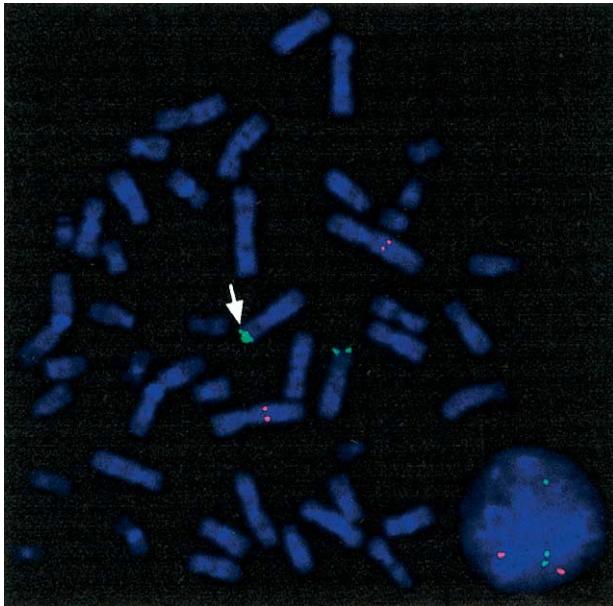
Figure 3   Two-color FISH analysis using PAC 135A7 (chromosome 6 [*green signal*]) and PAC 124L22 (chromosome 2 [*red signal*]). Montage of metaphase and interphase (*bottom right*) nuclei preparations from individual 13 is shown. One chromosome 6 homologue (*arrow*) displays a green signal of increased intensity, which, on the interphase, is shown as a double signal.

individual 13; 120 from individual 14) demonstrated that the green signal from PAC 135A7 was frequently duplicated, with the maximum separation of the two signals being the diameter of the signal (fig. 3).

The interphase nuclei were analyzed by scoring the number of distinct signals in each cell, with no attempt to assess the size of the signal. In no case were three or more widely separated signals seen. Thus, a score of three signals was most easily interpreted as two signals on one homologue and one signal on the other, and a score of four signals as two on each homologue (indicating a cell in G2). As expected in a culture not completely synchronized and where objects separated in three dimensions are viewed in two dimensions, there is considerable background variation in the number of signals seen per cell. The examples of three signals in one cell in the control individual or when the control probe was used are presumably either the result of failure to see the second signal on one homologue in a G2 cell (because of orientation within the nucleus) or an early stage of G2 when the replication is slightly asynchronous.

In spite of the background variation in the number of signals seen per cell, statistical analysis of the number of signals (table 3) gives a very clear result. In patient 13, the proportion of cells containing asymmetrical sig-

nals with the 6p25 probe (61%) is much greater than either that with the 2q21 probe (26%) ($\chi^2_1 = 30$; $P < .001$) or that observed in the control individual (31%) ($\chi^2_1 = 17$; $P < .001$). In the 74 control cells analyzed, the total number of signals from the two probes were virtually identical (190 for 6p25; 188 for 2q21), and equal numbers were asymmetrical. With the control probe 2q21, there is no difference, in the distribution of symmetrical and asymmetrical signals, between the patient and the control ($\chi^2_1 = 0.57$; $P < .49$). (The difference of distribution of signals between patient 13 and the control remains highly significant even if only those cells containing a symmetric 1:1 signal in 2q21 are considered [$\chi^2_1 = 15$; $P < .001$]; see table 4).

Very similar results were obtained with patient 14, scored for 120 cells. In this case, 69 (57%) of the 6p25 signals were asymmetrical, compared with 25 (21%) of the 2q21 signals ($\chi^2_1 = 34$; $P < .001$).

Discussion

This article has described a large pedigree with inherited iris hypoplasia and glaucoma that maps to 6p25 and in which direct sequencing has failed to demonstrate mutations in the known *FOXC1* gene. In four other pedigrees with a similar phenotype mapping to 6p25, direct sequencing of *FOXC1* has also not demonstrated mutations (Mears et al. 1998).

On the basis of the anomalous genotyping results observed with D6S967—in which the 18 affected individuals inherited three alleles, two of which were shared in all these individuals—we hypothesize that a duplication event on 6p25 is present in the affected members of this pedigree. Since the size of a duplicated tetranucleotide repeat is not under any evolutionary pressure to remain conserved, we believe that, after the duplication event occurred, replication slippage led to the creation of unequal-length alleles that have enabled

Table 3

Analysis of Total Counts of Signals from PAC 135A7 (6p25) and Control PAC 124L22 (2q21) in Individual 13 and Control

	Individual 13 ($n = 119$)		Control ($n = 74$)	
PAC used	6p25	2q21	6p25	2q21
No. of individuals:				
Symmetrical[a]	46	88	51	51
Asymmetrical[b]	73	31	23	23

[a] Equal numbers of signals on each homologue (i.e., 1 + 1 or 2 + 2).

[b] Unequal numbers of signals on each homologue (i.e., 1 + 2, 1 + a cluster of signals, or 2 + a cluster of signals).

Table 4

Analysis of 6p25 Probe Only in Those Cells in Which the 2q21 Probe Had Two Signals

	Individual 13	Control
No. symmetrical	30	34
No. asymmetrical	38	7

NOTE.—Data are as defined in the footnotes to table 3.

this duplication to be observed on a microsatellite gel. FISH of a PAC clone demonstrating a duplication on 6p25 that includes *FOXC1* confirms our interpretation of the genotyping data. The high number of cytogenetic abnormalities reported in this region (Davies et al. 1999; Sheffield et al. 1999) suggests that this location may be an area of genetic instability. The telomeric location, the GC-rich content, and the presence of multiple CCG repeats (Jones et al. 2000) within and around the *FOXC1* gene may also be contributing to the likelihood of such events. However, since this duplication is present in three living generations of this pedigree, it is highly probable that it represents a stable ancestral event.

One hypothesis to explain the genetic basis of iris hypoplasia in large pedigrees with mapping to 6p25 that do not contain *FOXC1* mutations is the existence of a second glaucoma gene, a hypothesis that mapping data support (Mears et al. 1998). Although we cannot exclude the involvement of a second gene, the demonstrated duplication involving *FOXC1* in a pedigree of this size strongly suggests that alterations in gene dosage of *FOXC1* causes ocular disease, especially since duplications of part of *FOXC1* have been shown to be pathogenic (Kawase et al. 2000). There are no published examples of chromosomal duplications causing either developmental anomalies or ocular pathology in humans, although chromosomal duplications do cause nondevelopmental conditions such as Charcot-Marie-Tooth disease (Lupski et al. 1991) and a variety of tumors (Weston et al. 1989).

The eye is known to be exquisitely sensitive to both reduced and increased gene dosage of key developmental genes. Increased expression of *PAX-6* resulting from an increased copy number has been shown to result in developmental ocular anomalies in transgenic mice (Schedl et al. 1996). *FOXC1* is believed to act as a transcription factor, and it is possible that haploinsufficiency caused by *FOXC1* mutations leads to altered expression patterns of target genes. We hypothesize that an altered pattern of gene expression arising from altered *FOXC1* gene dosage leads to the iris hypoplasia phenotype. The fact that the proportion of patients who develop glaucoma is much higher in this pedigree (100% of individuals who can be comprehensively examined) than in other *FOXC1*-related phenotypes (e.g.,

~50% in Axenfeld anomaly [Walter et al. 2000] suggests that increased dosage of *FOXC1* may result in a more severe phenotype than does reduced dosage. Further proof for this hypothesis could be obtained either by examining the phenotype in an animal model with an additional copy of *FOXC1* or by looking for increased *FOXC1* expression in ocular tissue derived from affected patients. Since most animal models require surgical treatment to induce glaucoma, such a transgenic system with early onset of the phenotype may prove to be particularly valuable. It would also be interesting to explore the possibility that some of the other families with mapping to 6p25 and in which *FOXC1* mutations have not been found may contain cytogenetic abnormalities that include the *FOXC1* gene but not any adjacent microsatellite markers. We are continuing this research by investigating this duplication by using physical mapping and strand FISH.

Acknowledgments

Electronic-Database Information

Accession numbers and URLs for data in this article are as follows:

Online Mendelian Inheritance in Man (OMIM), http://www.ncbi.nlm.nih.gov/Omim (for *PITX2* [MIM 601542], *MYOC* [MIM 601652], *CYP1B1* [MIM 601771], *LMX1B* [MIM 602575], and *FOXC1* [MIM 601090])

Research Genetics, http://www.resgen.com/index.php3

Whitehead Institute for Biomedical Research/MIT Center for Genome Research (http://www-genome.wi.mit.edu/)

References

Alward WLM, Kwon YH, Khanna CL, Hayreh SS, Johnson AT, Sheffield VC, Stone EM (2000) Prevalence of myocilin mutations in a large consecutive unselected series of open angle glaucoma patients and glaucoma suspects. Invest Ophthalmol Vis Sci 41:S526

Craig JE, Mackey DA (1999) Glaucoma genetics: where are we? where will we go? Curr Opin Ophthalmol 10:126–134

Davies A, Mirza G, Flinter F, Ragoussis J (1999) An interstitial deletion of 6p24-p25 proximal to the FKHL7 locus and including AP-2a that affects anterior eye chamber development. J Med Genet 36:708–710

Fox M, Povey S (2000) Fluorescent in situ hybridization (FISH) to mouse chromosomes. In: Jackson IJ, Abbott CM (eds) Mouse genetics and transgenics: a practical approach. Oxford University Press, London, pp 154–169

Jones C, Mullenbach R, Grossfeld P, Auer R, Favier R, Chien K, James M, Tunnacliffe A, Cotter F (2000) Co-localisation of CCG repeats and chromosome deletion breakpoints in Jacobsen syndrome: evidence for a common mechanism of chromosome breakage. Hum Mol Genet 9:1201–1208

Jordan T, Ebenezer N, Manners R, McGill J, Bhattacharya S (1997) Familial glaucoma iridogoniodysplasia maps to a 6p25 region implicated in primary congenital glaucoma and iridogoniodysgenesis anomaly. Am J Hum Genet 61:882–888

Kawase K, Kawase C, Udo M, Yoh M, Yamamoto T, Kitazawa Y, Fingert JH, Alward WLM, Stone EM, Semina EV (2000) Genetic variation in five glaucoma-related genes in Japanese patients with juvenile glaucoma and congenital glaucoma. Invest Ophthalmol Vis Sci 41:S824

Lathrop GM, Lalouel JM (1984) Easy calculations of lod scores and genetic risks on small computers. Am J Hum Genet 36:460–465

Lupski JR, de Oca-Luna RM, Slaugenhaupt S, Pentao L, Guzzetta V, Trask BJ, Saucedo-Cardenas O, Barker DF, Killian JM, Garcia CA (1991) DNA duplication associated with Charcot-Marie-Tooth disease type 1A. Cell 66:219–232

Mackey DA, Green CM, Sale MM, Craig JE, Dickinson JL, McCartney DL, Stanwix SH, Wong TL, McNaught AI (2000) Familial aggregation of glaucoma: experience with the glaucoma inheritance study in Tasmania (GIST). Invest Ophthalmol Vis Sci 41:S527

Mears AJ, Jordan T, Mirzayans F, Dubois S, Kume T, Parlee M, Ritch R, Koop B, Kuo WL, Collins C, Marshall J, Gould DB, Pearce W, Carlsson P, Enerback S, Morissette J, Bhattacharya S, Hogan B, Raymond V, Walter MA (1998) Mutations of the forkhead/winged-helix gene, FKHL7, in patients with Axenfeld-Rieger anomaly. Am J Hum Genet 63:1316–1328

Mirzayans F, Gould DB, Heon E, Billingsley GD, Cheung JC, Mears AJ, Walter MA (2000) Axenfeld-Rieger syndrome resulting from mutation of the FKHL7 gene on chromosome 6p25. Eur J Hum Genet 8:71–74

Morissette J, Falardeau P, Dubois S, Bergeron J, Vonck P, Coté G, Anctil J-L, Amyor M, Blondeau P, Bergeron E, Raymond V (1997) A common gene for developmental and familial open-angle glaucomas confined on chromosome 6p25. Am J Hum Genet Suppl 61:A286

Nishimura D, Swiderski R, Alward W, Searby CC, Patil SR, Bennet SR, Kanis AB, Gastier JM, Stone EM, Sheffield VC (1998) The forkhead transcription factor gene FKHL7 is responsible for glaucoma phenotypes which map to 6p25. Nat Genet 19:140–147

Quigley HA (1996) Number of people with glaucoma worldwide. Br J Ophthalmol 80:389–393

Schedl A, Ross A, Lee M, Engelkamp D, Rashbass P, van Heyningen V, Hastie ND (1996) Influence of PAX6 gene dosage on development: overexpression causes severe eye abnormalities. Cell 86:71–82

Sheffield VC, Nishimura DY, Kanis AB, Walton DS, Alward WL, Stone EM (1999) Gene dosage of the FKHL7 gene causes defects of the anterior chamber of the eye. Invest Ophthalmol Vis Sci 40:S596

Walter MA, Kulak KC, Héon E, Ritch R, Pearce WG, Damji KF, Allingham RR, Shields MB (2000) Comparison of genotype with glaucoma incidence and treatment in Axenfeld-Rieger patients. Invest Ophthalmol Vis Sci 41:S527

Weston A, Willey JC, Modali R, Sugimura H, McDowell EM, Resau J, Light B, Haugen A, Mann DL, Trump BF (1989) Differential DNA sequence deletions from chromosomes 3, 11, 13, and 17 in squamous-cell carcinoma, large-cell carcinoma, and adenocarcinoma of the human lung. Proc Natl Acad Sci USA 86:5099–5103

Wolfs RC, Klaver CC, Ramrattan RS, van Duijn CM, Hofman A, de Jong PT (1998) Genetic risk of primary open-angle glaucoma. Arch Ophthalmol 116:1640–1645